Published in final edited form as:
Dev Biol. 2007 December 1; 312(1): 384–395.

Tgfb1 expressed in the *Tgfb3* locus partially rescues the cleft palate phenotype of *Tgfb3* null mutants

Liang-Tung Yang and **Vesa Kaartinen***
Developmental Biology Program, The Saban Research Institute of Childrens Hospital Los Angeles, Departments of Pathology and Surgery, Keck School of Medicine, University of Southern California, Los Angeles, CA 90027, USA.

Abstract

Although TGF-β isoforms (TGF-β1-3) display very similar biochemical characteristics *in vitro*, it has been determined that they demonstrate different or even opposing effects *in vivo*. During embryogenesis, TGF-βs play important roles in several developmental processes. *Tgfb3* is strongly expressed in the prefusion palatal epithelium, and mice lacking *Tgfb3* display a cleft of the secondary palate. To test whether the effect of TGF-β3 in palatogenesis is isoform-specific *in vivo*, we generated a knockin mouse by replacing the coding region of exon1 in the *Tgfb3* gene with the full length *Tgfb1* cDNA, which resulted in the expression of *Tgfb1* in the *Tgfb3* expressing domain. The homozygote knockin mice display a complete fusion at the mid-portion of the secondary palate, while the most anterior and posterior regions fail to fuse appropriately indicating that *in vivo* replacement of TGF-β3 with TGF-β1 can only partially correct the epithelial fusion defect of *Tgfb3* knockout embryos. Palatal shelves of *Tgfb1* knockin homozygote mice adhere, intercalate, and form characteristic epithelial triangles. However, decreased apoptosis in the midline epithelium, slower breakdown of the basement membrane and a general delay in epithelial fusion were observed when compared to control littermates. These results demonstrate an isoform-specific role for TGF-β3 in the palatal epithelium during palate formation, which cannot be fully substituted with TGF-β1.

Keywords

TGF-β; palatogenesis; cleft palate; Transforming growth factor; development; mouse

Introduction

Cleft palate and cleft lip are among the most common congenital birth defects in humans occurring once in every 500-700 births (Murray, 2002;Rice, 2005). While our understanding of molecular control of palate formation (=palatogenesis) has greatly improved during the last decade, many questions still remain unanswered (Chai and Maxson, Jr., 2006;Schutte and Murray, 1999). The mammalian secondary palate develops from bilateral outgrowth of palatal shelves from the maxillary processes. Two key cell types underlying palatogenesis are epithelial cells derived from the pharyngeal ectoderm and mesenchymal cells derived mostly from the neural crest (Dudas and Kaartinen, 2005;Gritli-Linde, 2007;Schutte and Murray, 1999). The interactions between the ectoderm and the underlying mesenchyme promote the vertical growth of palatal shelves beside the tongue. Accompanied by the enlargement of the

*Corresponding author: vkaartinen@chla.usc.edu

lower jaw and forward displacement of the tongue, palatal shelves elevate to a horizontal position above the tongue. Subsequently, they make contact, become adherent, and fuse (Ferguson, 1988).

Many growth factors, signaling pathways and nuclear factors have been implicated in palatogenesis (Dudas and Kaartinen, 2005;Gritli-Linde, 2007;Hilliard et al., 2005). Among them, TGF-βs have been shown to play important roles in regulating epithelial-mesenchymal interactions leading to appropriate growth and fusion of palatal shelves (Nawshad et al., 2005); *Tgfb2* is expressed in the palatal mesenchyme, whereas *Tgfb1* and *Tgfb3* expression was proposed to be limited to the pre-fusion palatal midline epithelium (Fitzpatrick et al., 1990;Pelton et al., 1990). Both *Tgfb2* and *Tgfb3* knockout mice display cleft palate phenotypes, which are caused by different pathogenetic mechanisms (Kaartinen et al., 1995;Martinez-Alvarez et al., 2000;Proetzel et al., 1995;Sanford et al., 1997;Taya et al., 1999). Palatal shelves of *Tgfb2* knockout mice fail to grow and elevate, suggesting a role for TGF-β2 in the growth of the palatal mesenchyme. Interestingly, palatal shelves of *Tgfb3* knockout mice elevate and become apposed, but fail to fuse leading to cleft palate. Although TGF-β1 is also expressed in the epithelial tips of prefusion palatal shelves, *Tgfb1* null mutants do not display a cleft palate phenotype (Kulkarni et al., 1993;Shull et al., 1992).

TGF-β isoforms share a high degree of homology in the mature domain of the growth factor and are qualitatively indistinguishable in *in vitro* cell culture assays (Roberts and Sporn, 1992). During embryogenesis, TGFβ isoforms display overlapping but distinct expression patterns, and they are often expressed at sites where commitment of a specific cell fate occurs (Akhurst et al., 1990;Pelton et al., 1990). Non-overlapping phenotypes associated with the null mutation of different TGF-β isoforms suggest that biological activities of TGF-β isoforms may be different *in vivo*. Indeed, functional analyses of the TGF-β isoforms *ex vivo* have revealed that they have different, or even opposing, biological activities in certain model systems (Foitzik et al., 1999;Li et al., 1999;Shah et al., 1995). In a skin organ culture model, TGF-β1 treatment resulted in the inhibition of hair follicle development and keratinocyte proliferation, whereas TGF-β2 treatment potently stimulated hair follicle formation and concomitantly produced epidermal hyperplasia (Foitzik et al., 1999). In skin grafts, TGF-β3, but not TGF-β1, was shown to protect keratinocytes against TPA-induced cell death (Li et al., 1999). Moreover, in a rat cutaneous wound healing model, TGF-β1 and TGF-β2 were shown to be involved in cutaneous scarring, while TGF-β3 acted as an anti-scarring agent (Shah et al., 1995).

In this study, we tested whether the role of TGF-β3 *in vivo* during palatal fusion is isoform specific by replacing the coding region of exon1 in the *Tgfb3* gene with *Tgfb1* cDNA using gene-targeting technology. The resulting *Tgfb1*-knockin (*Tgfb1*-KI) mice, which express *Tgfb1* in the *Tgfb3* locus and are null for *Tgfb3*, displayed a remarkable improvement in the cleft palate phenotype when compared to *Tgfb3* null mutants. A mid-portion of the secondary palate demonstrated a complete fusion while the anterior secondary palate still failed to fuse to the primary palate, and the posterior palate displayed a submucous cleft. The rate of apoptosis was attenuated and breakdown of the basement membrane was reduced in *Tgfb1*-KI samples when compared to wild-type littermates. These findings demonstrate a partial isoform-specific role for TGF-β3 in the palatal epithelium during the development, which cannot be fully compensated by TGF-β

Materials and Methods

Gene targeting of *Cre* cDNA into *Tgfb3* locus (*Tgfb3*-Cre mice)

A targeting vector was generated by combining a 9-kb clone isolated from the B6xCBA (F1) mouse genomic library (right arm), a 1.6- kb PCR fragment amplified from the R1-ES cell

DNA (left arm), and a cassette containing a promoterless Cre gene and a neomycin-resistant gene driven by the phosphoglycerate kinase promoter (PGK-Neo) to replace the coding region of the ATG containing exon 1 of the *Tgfb3* gene. Briefly, a 1.6-kb PCR-amplified 5' XbaI-BamHI genomic fragment, the Cre-pgk-Neo, and a 10-kb 3' NotI-EcoRI genomic fragment (generated by fusing a 2.6-kb Not1-Kpn1 PCR fragment with a 7.6-kb KpnI-EcoRI fragment from the library clone) containing exons 2 and 3 were subcloned into the pKOdt plasmid (Stratagene). R1-ES cells were cultured, electroporated and screened as previously described (Kaartinen et al., 1995;Kaartinen et al., 2004). Targeted colonies were initially identified by PCR amplification of a 2-kb fragment using a 5'-arm outside sense primer1 (GCATGCTCCAGACTGCCTTGGGA) and a Cre anti-sense primer 2 (CCTCATTCACTCGTTGCATCGACCGG). Southern blot analyses of genomic DNAs, digested with both ClaI and KpnI, were used to confirm homologous recombination of the targeted allele using the Cre and Neo probes. A total of 7 positive homologous recombinant ES cells clones were obtained from 260 G418-resistant clones. ES cells from two independent targeted clones were microinjected into C57/BL6J blastocysts by the transgenic core facility at the University of Southern California. Three male chimeras (male/female ratio was 9:3) were used to produce heterozygote *Tgfb3-Cre* mice.

Gene targeting of *Tgfb1* cDNA into *Tgfb3* locus (*Tgfb1*-KI mice)

A 1.6-kb PCR-amplified XbaI-BamHI *Tgfb3* genomic fragment, a *Tgfb1* cDNA with phosphoglycerate kinase (pgk) polyA sequence, a loxP-floxed neomycin-resistant gene driven by the pgk promoter, and a 10-kb PCR-amplified NotI-EcoRI genomic fragment containing exons 2 and 3 of *Tgfb3* gene were subcloned into a pKOdt vector (Stratagene). Targeted colonies were initially identified by PCR amplification of a 2-kb fragment using a 5'-arm outside sense primer 1 (GCATGCTCCAGACTGCCTTGGGA) and a *Tgfb1* anti-sense primer 3 (GGAGTGGGAGCAGAAGCGGCAGTAGCC). Southern blot analysis of genomic DNAs digested with NheI was used to confirm homologous recombination of the targeted allele using a Neo probe. One positive homologous recombinant ES cell clone was obtained from 192 G418-resistant clones. This cell line produced two highly chimeric males, both of whom were germ line transmitters.

Mouse breeding, embryo isolation, and genotype assays

ROSA26 Cre reporter mice were obtained from the Jackson laboratory (Bar Harbor, ME, USA). *Tgfb3* −/− mice were previous made in the laboratory (Kaartinen et al., 1995). *Tgfb3-Cre* and *Tgfb1-K* mice were generated as described above. All mice were bred to have a mixed genetic background. Mice were mated during the dark period of the controlled light cycle and female mice acquiring vaginal plugs were designated as day 0. At the time interval indicated in respective figures (E14 to E17), females were euthanized by CO_2 and embryos were collected in PBS (Invitrogen) followed by further analyses. All studies and procedures performed on mice were carried out at the Animal Care Facility of the Saban Research Institute, and were approved by the CHLA Animal Care and Use Committee (IACUC). Mice tail biopsies were collected and genotyped by PCR. For the *Tgfb1*-KI allele the following oligos were used; sense: GAGTCAGAGCCCGGCAGAACCTGTT, antisense: GCCGGTTACCAAGGTAACGCCAGGA. Oligos for genotyping *Cre* and *Tgfb3*-null alleles have been described elsewhere (Kaartinen et al., 2004;Shi et al., 1999).

Histological analyses, X-gal staining, scanning electron microscopy and *In situ* Hybridization

Mouse embryos or tissues were fixed in 4% formaldehyde for 24 h, and paraffin sections were stained with hematoxylin-eosin using standard procedures. Frozen sections of embryos were stained for lacZ activity as described (Hogan et al., 1994). For scanning electron microscopy analysis, samples were fixed in 4% formaldehyde plus 0.5% glutaraldehyde for 48 hours and

processed at the Tissue Imaging Core in DEI/USC Norris Cancer Center. Pictures were recorded using a scanning electron microscope with computerized digital capture (Hitachi S-570). RNA *in situ* hybridization was performed as previous described (Moorman et al., 2001). A 455-bp fragment of the mouse *Tgfb1* cDNA (nts 206-661) was subcloned into pBSks, digested with KpnI, and transcribed with T3 RNA polymerase to prepare the anti-sense probe, according to the manufacturers' protocol (Boehringer Mannheim).

Organ culture, immunostainings, and TUNEL assays

Palatal shelves were cultured for 48 hours in BGJb medium (Invitrogen) (Kaartinen et al., 1997) and analyzed with serial sectioning. Paraffin sections were stained for both laminin and K14 using an anti-laminin antibody (1:250, Sigma) and an anti-K14 antibody (1:250, Lab Vision) (Harlow E and Lane D, 1988). Images from the anti-laminin staining (red color) and the anti-K14 staining (green color) were superimposed using Adobe Photoshop software. Immunostaining for phospho-Smad2/3 was done in paraffin sections using Phospho-Smad2 Ser465/467 antibody (1:200, Chemicon), after antigen retrieval by boiling in 10 mM Tris buffer (pH 10). Apoptotic cells were detected in paraffin sections using DeadEnd Fluorometric TUNEL system (Promega).

Western Blotting

Tips of palatal shelves were dissected out from E14 embryos (n=3 for each genotype) and frozen in an ethanol-dry ice bath. Samples were lysed at 90°C for 10 minutes in 40 μl 1%SDS buffer (50 mM Tris pH 7.5, 1% SDS, 1 mM EDTA, 10% Glycerol) plus protease inhibitors (Aprotinin 2μg/ml, Leupeptin 20μg/ml, Pepstatin A 1μM, PMSF 1 mM) and phosphatase inhibitors (NaF 10 mM, Sodium Vanadate 1mM). Five μg of protein per lane was resolved by 9% SDS PAGE and electroblotted onto PVDF membrane (Hybond-P, Amersham). The membrane was blocked and incubated either overnight at 4°C with diluted anti-phospho Smad2 antibody (Cell signaling, 1:1000 dilution in blocking solution) or 1 hour with diluted anti-Smad2 antibody (Zymed, 1:500 dilution in blocking buffer). The membrane was then probed with horseradish peroxidase (HRP)-conjugated goat anti-rabbit antibody and developed with HRP substrate (Immobilon Western, Millipore). The chemiluminescent signal was exposed to X-ray films and the signal intensity was quantified by densitometric analysis using Un-Scan it Gel software (Silk Scientific, Inc.). Signal intensities of phospho-Smad2/3 bands from wild-type and mutant samples were normalized to signal intensities of Smad2, using the total pixel value obtained by the ‘Un-Scan it’ gel software.

Total RNA preparation, reverse transcription, and gene expression analyses

Total RNA was isolated from tips of E14 palatal shelves using the RNeasy mini kit (Qiagen), and cDNAs were synthesized using the Omniscript reverse transcription kit (Qiagen) according to the manufacturers' protocols. Real-time PCR was carried out using a LightCycler 1.5 (Roche) with the LightCycler Taqman Master mix and universal probe/primer sets for the following genes: *Tgfb1* (mouse universal probe #72, Left primer TGGAGCAACATGTGGAACTC, and right primer GTCAGCAGCCGGTTACCA), *Tgfb3* (mouse universal probe #25, left primer CCCTGGACACCAATTACTGC, and right primer TCAATATAAAGGGGGCGTACA), *Mmp-13* (mouse universal probe # 62, left primer CAGTCTCCGAGGAGAAACTATGA, and right primer GGACTTTGTCAAAAAGAGCTCAG), and *β-actin* (universal probe #106, left primer TGACAGGATGCAGAAGGAGA, and right primer CGCTCAGGAGGAGCAATG). Relative quantification of gene expression between samples, and absolute quantification of gene expression within a sample were done using the LightCycler software 4.0. The amplification efficiencies, which were calculated from standard curves generated by dilutions of cDNA samples at known concentrations; for *Tgfb1*, *Tgfb3*, and *β-actin*, were 1.803, 1.911, and 1.742, respectively.

CHO cell transfection and luciferase reporter assay

The mouse TGF-β1 cDNA was purchased from ATCC (#3586216), PCR-amplified, and cloned into the pGK plasmid. Three independent bacterial clones were chosen to transfect the CHO cells using lipofectamine 2000 (Invitrogen). The supernatant from transfected cells was diluted with an equal volume of DMEM and applied to MLE cells stably integrated with plasminogen activator inhibitor-1/luciferase reporter plasmid. Luiciferase activity was measured by using the Luciferase Reporter Assay System (Promega) with a Luminometer.

Results

Generation of *Tgfb1*-KI and control *Tgfb3*-Cre mice

To test whether TGF-β1 is able to substitute for TGF-β3 when expressed *in vivo* in the *Tgfb3*-expressing domain, we used gene targeting to replace the coding region in exon 1 of the *Tgfb3* gene with a full-length cDNA encoding the mouse *Tgfb1* gene followed by the *loxP-Pgk-Neo-loxP* cassette (Fig. 1A). Since the *Tgfb1*-KI allele lacks the sequences encoded by *Tgfb3* exon 1, and since all the promoter and regulatory elements of the *Tgfb3* gene were essentially preserved, we predicted that i) *Tgfb1* expression would faithfully recapitulate the endogenous expression pattern of the *Tgfb3* gene and ii) the *Tgfb1*-KI allele would be a true null allele for *Tgfb3*. First, we verified that our PCR-generated mouse *Tgfb1* cDNA clones produced a biologically active ligand. Culture media collected from CHO cell cultures transfected with the *Tgfb1* expression vector were analyzed by the plasminogen activator inhibitor-1/luciferase reporter assay (Abe et al., 1994). The positive clone #1 was used to construct the targeting vector, which in turn was used to generate chimeric mice and subsequently mice heterozygous for the *Tgfb1* knockin allele (*Tgfb1*-KI) (Fig. 1C).

To prove that the generated *Tgfb1*-KI allele is a true null allele for *Tgfb3,* and that a resultant phenotype is due to an *in vivo* replacement of TGF-β3 with TGF-β1, we generated another mouse line by inserting the promoterless *Cre* recombinase-*Pgk-Neo* cassette into *Tgfb3 exon1* by homologous recombination essentially as described above for the *Tgfb1* knockin allele (Fig. 1A). Concordant with the published expression pattern for *Tgfb3* (Fitzpatrick et al., 1990;Pelton et al., 1990), Cre-induced recombination was strikingly strong in the prefusion palatal epithelium (Fig. 1D). Moreover, the homozygote *Tgfb3-Cre* mice displayed a cleft palate phenotype identical to that of the previously described *Tgfb3* knockout mice (Kaartinen et al., 1995;Proetzel et al., 1995) confirming that homozygous *Tgfb3*-Cre mice were true null mutants for the *Tgfb3* gene, and suggesting that the analogous *Tgfb1*-KI allele is a true null allele (Fig. 2).

In vivo replacement of TGF-β3 with TGF-β1 leads to a partial rescue of the *Tgfb3*- null cleft palate phenotype

Crossing the *Tgfb1*-KI heterozygote male mice with heterozygote female mice produced an expected Mendelian ratio of wild-types, heterozygotes and homozygotes at E14 (n=103) and at E17 (n=36). However, the homozygote knockin mice failed to suckle as demonstrated by a complete lack of milk in the stomach (data not shown). At two weeks of age we could not detect any surviving homozygote *Tgfb1*-KI mice (n=45). While a superficial macroscopic examination of the homozygote *Tgfb1*-KI newborn mice failed to demonstrate any obvious cleft palate phenotypes, detailed scanning electron microscopy and histological analyses exposed a submucous posterior cleft and a failure of the primary palate to fuse to the secondary palate (Fig 2). It is noteworthy that while the nasal septum failed to fuse with the anterior palate in homozygote *Tgfb1* knockin embryos, a large segment of the mid-palate displayed complete epithelial fusion with continuous palatal mesenchyme; a phenotype seen in neither conventional *Tgfb3* knockouts (Kaartinen et al., 1995;Proetzel et al., 1995) nor epithelial specific *Tgfb* receptor knockouts (Dudas et al., 2006;Xu et al., 2006).

Tgfb1 is strongly expressed in the tips of palatal shelves in *Tgfb1* knockin mice

The partial rescue seen in the *Tgfb1* knockin mice could result from a failure to achieve an appropriate expression level of *Tgfb1* in the knockin mice. Therefore, we first carefully quantified *Tgfb1* and *Tgfb3* mRNAs in developing palates of embryos derived from the crossing of *Tgfb1*-KI heterozygote mice. The tissues composed of both the palatal epithelium and mesenchyme were dissected from distal tips of prefusion palatal shelves of wild-type, *Tgfb1*-KI heterozygote and homozygote embryos at E14 (Fig. 3A). Total RNA was isolated and reverse-transcribed, and the obtained cDNA was then quantified using the TaqMan real-time PCR approach (Fig. 3B). In embryos heterozygous for both the *Tgfb1* knockin and the endogenous *Tgfb3* alleles, the level of *Tgfb1* mRNA in the distal edges of palatal shelves was approximately 50% higher, and the level of *Tgfb3* mRNA was approximately 2-fold lower, than the level in corresponding wild-type samples. In contrast, in homozygous *Tgfb1*-KI mice, there was no detectable *Tgfb3* expression, while the level of *Tgfb1* mRNA was approximately 2-fold higher than that in the corresponding wild-type sample. These results indicated that mice with the *Tgfb1* knockin allele can express *Tgfb1* mRNA under the control of the endogenous *Tgfb3* promoter.

Next, we dissected tips of prefusion palatal shelves at E14.0 as outlined above and analyzed them using qPCR with an absolute quantification method to compare *Tgfb1* and *Tgfb3* expression levels in wild-types and *Tgfb1*-KI heterozygotes. Based on standard curves, absolute quantification revealed that the total level of *Tgfb3* expression in wild-type palatal shelves was about 3-fold higher than that of *Tgfb1* (Fig. 3C). An absolute quantification assay for *Tgfb1* and *Tgfb3* mRNA expression was also applied to the *Tgfb1*-KI heterozygote samples and the result indicated that *Tgfb1* mRNA was expressed at a level about 2.5-fold higher than *Tgfb3* mRNA (Fig. 3D). In summary, these analyses revealed that the failure of palatal shelves to fuse appropriately in the homozygote samples was not caused by defective global expression of *Tgfb1* at the edges of the prefusion palatal shelves.

To verify that the fusion failure in the anterior and posterior palate was not a result of regional defects in *Tgfb1* expression, we performed *in situ* hybridization analyses on serial sections of the control and *Tgfb1*-KI homozygote embryos at three different levels (Fig. 3E). The hybridization signal detected in the palatal epithelium was stronger in the homozygote knockin samples than in control samples, and demonstrated comparable intensity along the entire anterior-posterior axis.

Tgfb1-KI homozygotes and wild-type controls display a comparable level of canonical TGF-β signaling activity

Upon TGF-β binding, TGF-β type II receptors, which are constitutively active, are brought into a complex with type I receptors and subsequently activate type I receptors, resulting in the phosphorylation and activation of intracellular effectors Smad2 and Smad3. To confirm that the *Tgfb1*-KI allele generated a functional TGF-β1 protein, we analyzed the phosphorylation level of Smads2 and -3 (pSmad2/3) in the midline epithelium of E14 palatal shelves from wild-type, *Tgfb3*-Cre homozygote, and *Tgfb1*-KI homozygote embryos by immunostaining with an anti-pSmad2/3 antibody (Fig. 4). The pSmad2/3-positive staining was seen in the periderm and midline epithelium in wild-type and *Tgfb1*-KI homozygote embryos, whereas staining in the midline epithelium of *Tgfb3*-Cre homozygote embryos was barely detectable. Importantly, we did not observe any significant differences in the phosphorylation level of Smad2/3 in the midline epithelium between wild-type and *Tgfb1*-KI homozygote embryos in the anterior, mid- or posterior palate (Fig. 4A). In addition, we dissected tips of prefusion palatal shelves from wild-type, *Tgfb1*-KI and *Tgfb3*-Cre homozygote embryos and analyzed their Smad2/3 phophorylation levels using a quantitative western blot analysis (Fig. 4B and C). While phosphorylation between wild-type and *Tgfb1*-KI samples was comparable, the homozygote

Tgfb3-Cre samples consistently displayed about 10% reduction in phosphorylation, when compared to the wild-type controls or *Tgfb1*-KI samples. The relatively strong, albeit reduced Smad2/3 phosphorylation in *Tgfb3* null mutant samples is likely due to the fact that most of the cells in the harvested tissues were of mesenchymal origin, which also exhibit phosphorylated Smad2/3, as can be seen in Fig. 4A. To conclude, these results suggest that the *Tgfb1*-KI allele can express a functional protein, and that *in vivo* replacement of TGF-β3 with TGF-β1 results in a comparable level of canonical TGF-β signaling activity.

Palatal shelves *of Tgfb*1-KI homozygote mice display a delayed fusion

Palatal shelves isolated from mice lacking TGF-β type I or type II receptors in the palatal epithelium, as well as palatal shelves from *Tgfb3* −/− mice, display an persistent intact midline seam under organ culture conditions (Dudas et al., 2006;Kaartinen et al., 1997;Taya et al., 1999;Xu et al., 2006). To more closely compare the fusion of palatal shelves between *Tgfb1*-KI and control mice, we dissected prefusion palatal shelves from control and mutant embryos and cultured them under chemically defined conditions in the air-medium interface for 48 hours. The control samples demonstrated an almost complete fusion characterized by a loss of epithelial cells in the midline region (Fig. 5A, C, E, G). In contrast, the *Tgfb1*-KI samples displayed a midline seam that was only partially degraded displaying a patchy loss of epithelial cells (Fig. 5B, D, F, H). Interestingly, the basement membrane was still clearly visible even in locations where epithelial cells were lost, as demonstrated by immunostaining for the basement membrane marker (laminin) and for the epithelial cell marker (cytokeratin-14) (Fig. 5I-K). To conclude, our organ culture analyses reveal that the fusion process is significantly delayed in knockin samples when compared to controls despite the fact that *Tgfb1*-KI samples demonstrate a seemingly normal successful fusion in the mid-palate *in vivo*.

It has been previously suggested that the disappearance of midline epithelium requires intensive remodeling of the extracellular matrix, and that one of the key enzymes in this process is matrix metalloproteinase-13 (MMP-13), the expression of which is upregulated in the midline epithelium seam and the surrounding mesenchyme during palatal fusion (Blavier et al., 2001). In *Tgfb3* knockout mice, *Mmp-13* expression domain is greatly reduced during palatogenesis, suggesting that its expression is controlled by TGF-β3 (Blavier et al., 2001). Therefore, we compared *Mmp-13* expression in the tips of palatal shelves between wild-type and *Tgfb1*-KI samples (Fig. 5L). Our quantitative real-time PCR analysis demonstrated that misexpression of *Tgfb1* in the *Tgfb3* locus failed to restore *Mmp-13* expression in *Tgfb1*-KI homozygous samples to the level seen in wild-type littermates.

Palatal shelves of *Tgfb1*-KI homozygotes become adherent but display reduced apoptosis in the midline palatal epithelium during palatal fusion

Previous studies have emphasized the importance of intercalation of the apposing epithelia as a necessary initial step during palatal fusion (Martinez-Alvarez et al., 2000), and apoptosis as a main mechanism for the removal of the midline epithelium during subsequent stages of palatogenesis (Cuervo et al., 2002). Therefore, we examined both the histology and apoptosis of the midline epithelium seam during the fusion in *Tgfb1*-KI homozygote, *Tgfb3*-Cre homozygote, and control embryos (Fig. 6). Histological analysis of frontal sections showed that apposing palatal shelves of control and *Tgfb1*-KI homozygote samples became adherent, and that the midline epithelia were able to intercalate and form comparable oral and nasal epithelial triangles. In contrast, palatal shelves of *Tgfb3*-Cre homozygote samples made contact, but failed to intercalate and form epithelial triangles. TUNEL assays showed that control samples exhibited a large number of apoptotic cells, particularly in the nasal and oral epithelial triangles along the anterior-posterior axis, while a number of apoptotic nuclei were clearly detectable, but notably reduced in *Tgfb1*-KI samples. As a negative control, *Tgfb3*-Cre homozygote samples did not show any TUNEL-positive cells. Therefore, attenuated apoptosis

rather than reduced adherence likely accounts for the delayed fusion of *Tgfb1*-KI palatal shelves.

Discussion

During palatogenesis, TGFβ signaling is involved in the appropriate growth of palatal shelves and disappearance of the midline epithelial seam (Hay, 1995;Nawshad et al., 2004;Shuler, 1995;Young et al., 2000). Despite specific expression of both the *Tgfb1* and *Tgfb3* genes in distal edges of the prefusion palatal shelves, particularly in the medial edge epithelium, endogenously expressed *Tgfb1* is not able to rescue the cleft palate phenotype caused by the lack of *Tgfb3*. Yet, mice heterozygous for the *Tgfb3*-null allele have normal palate formation. Whether this failure to rescue the *Tgfb3* null phenotype was due to *in vivo* isoform-specific effects or simply reflected a significant difference in gene expression was not previously known. Given that three specific isoforms of TGF-β exhibit distinct and also overlapping expression patterns during development of different organs, we believe that use of the endogenous *Tgfb3* locus to express *Tgfb1* is the most reliable strategy to address the question of functional interchangeability.

Mice homozygous for *Tgfb3-Cre* allele displayed a cleft palate phenotype identical to that of the previously described *Tgfb3* knockout mice. Since an identical strategy was used to generate the *Tgfb1*-KI and *Tgfb3-Cre* alleles, it can be deduced that the *Tgfb1*-KI allele is also a true null allele for *Tgfb3,* and that the partially fused palatal phenotype in *Tgfb1*-KI embryos is due to *in vivo* replacement of TGF-β3 with TGF-β1. Moreover, we demonstrated that *Tgfb1* knockin allele can express *Tgfb1* mRNA under the control of the endogenous *Tgfb3* promoter by analyzing the level of *Tgfb1* and *Tgfb3* mRNA expression in distal tips palatal shelves isolated from wild-type, *Tgfb1*-KI heterozygote and homozygote embryos. In addition, our real-time absolute quantitative PCR data showed that *Tgfb1* was expressed at an approximately 2.5-fold higher level than *Tgfb3* in heterozygote *Tgfb1*-KI mice. Given that a total level of *Tgfb3* expression in wild-type palatal shelves was about 3-fold higher than that of *Tgfb1,* quantitative PCR data of Tgfb1-KI heterozygote samples reveal that *Tgfb1* mRNA expressed in distal edges of prefusion palatal shelves in homozygote *Tgfb1*-KI embryos is at a comparable level to that of *Tgfb3* in wild-type embryos. Furthermore, we detected similar phospho-Smad2/3 levels in midline epithelium between wild-type and *Tgfb1*-KI homozygote embryos. Taken together, our experiments indicate that the failure of TGF-β1 to fully substitute for the function of TGF-β3 in palatogenesis does not result from an inadequate level of gene expression and subsequent protein synthesis.

Our *in vivo* and *in vitro* experiments suggest that the fusion process is delayed in *Tgfb1*-KI homozygotes, leading to a partially fused palatal phenotype. During palatogenesis, the mid-anterior portion of palatal shelves make contact first, and the anterior and posterior parts come in contact later, displaying slightly rounded contact surface between the two opposing palatal shelves (Dudas and Kaartinen, 2005). As the fusion progresses, the midline epithelial seam gradually disappears along the sites where contact was first established, leading to a tighter contact between the opposing shelves and enabling closer contact between other parts of the palate. Delayed epithelial fusion in *Tgfb1*-KI samples, characterized by attenuated apoptosis and slower breakdown of the basement membrane, may provide a scenario for an *in vivo* situation, where the anterior and the posterior parts of the midline seam are insufficiently degraded, such that palatal shelves become stretched by a lateral growth of the head, resulting in the anterior cleft and the posterior submucous cleft. However, our present do not rule out the possibility that TGF-β3 plays an isoform-specific role in the most anterior and posterior regions of the palate. Interestingly, it has been reported that addition of TGF-β3 induced the formation of filopodia-like structures in the palatal epithelium in vitro, while TGF-β1 and TGF-β2 were relatively inefficient in inducing filopodia, but rather induced lamellipodia in organ

cultures (Taya et al., 1999). Perhaps, filopodia-like structures, which are more efficiently produced by TGF-β3 play a particularly significant role in the fusion of these regions, which fail to fuse in *Tgfb1-KI* embryos.

Mice deficient in TGF-β3, including both the traditional *Tgfb3* knockout mice (Kaartinen et al., 1995;Proetzel et al., 1995) and the new *Tgfb3-Cre* knockin mice described in this study, display either complete clefting of the secondary palate, or posterior clefting and superficial anterior adherence. A spectrum of cleft palate phenotypes can also be seen in humans; these vary from a total cleft to a submucous posterior cleft, and even to bifid uvula, which can be viewed as the mildest form of oral fusion defects (Dudas and Kaartinen, 2005). The etiology of these conditions is currently not well understood. We demonstrated that *in vivo* replacement of TGF-β3 with TGF-β1 results in a consistent mild cleft phenotype, characterized by an anterior small cleft and a posterior submucous cleft. At the molecular level, the knock-in TGF-β1 can restore the Smad-dependent TGF-β signaling activity in the *Tgfb3*−/− background, while it cannot resore the *Mmp13* level to that of the wild-type littermate. Despite the fact that TGF-β1 exerted an opposing effect to TGF-β3 in a rat cutaneous model (Shah et al., 1995), the partially rescued cleft palate phenotype seen in *Tgfb1*-KI homozygotes demonstrates that TGF-β1 and -β3 have partially overlapping functions in the palatal epithelium. This is consistent with earlier studies, which have demonstrated that addition of TGF-β1 or TGF-β2 can induce an almost complete fusion of *Tgfb3*−/− palatal shelves in organ cultures *in vitro* (Taya et al., 1999). Taken together data from our present study suggest that mildly perturbed developmental signals may lead to less severe cleft palate phenotypes. Since mice lacking both alleles of *Tgfb1* do not exhibit a cleft palate phenotype, it would be of interest to know, what is the role of TGF-β1 in the prefusion palatal epithelium? TGF-β1 may play an auxiliary role secondary to TGF-β3 during palatogenesis by fine-tuning the signaling field setup by TGF-β3, or it may compensate for the haploid deficiency of *Tgfb3* since *Tgfb3* heterozygotes do not display cleft palate. However, there may be cell type-specific differences in the processing and activation of TGF-β precursors, which may, in part, explain the observed differences between the effects of TGF-β1 and -β3 in the palatal epithelium.

To conclude, our experiments demonstrate that TGF-β isoforms display cell type specific differences during palatogenesis *in vivo*. We propose that in some cell types overlapping expression patterns may modulate the strength of signaling rather than create a field for signal specificity, while in other cell types, e.g., the palatal epithelium, there can be notable differences between the action of different isoforms.

Acknowledgements

We thank A. Nagy for technical assistance. LTY was supported by a grant from the CIRM (T2-00005) and VK by grants from the NIH (HL074862 and DE013085).

Reference List

Abe M, Harpel JG, Metz CN, Nunes I, Loskutoff DJ, Rifkin DB. An assay for transforming growth factor-beta using cells transfected with a plasminogen activator inhibitor-1 promoter-luciferase construct. Anal. Biochem 1994;216:276–284.

Akhurst RJ, Fitzpatrick DR, Gatherer D, Lehnert SA, Millan FA. Transforming growth factor betas in mammalian embryogenesis. Prog. Growth Factor Res 1990;2:153–168. [PubMed: 2132953]

Blavier L, Lazaryev A, Groffen J, Heisterkamp N, DeClerck YA, Kaartinen V. TGF-beta3-induced palatogenesis requires matrix metalloproteinases. Mol. Biol. Cell 2001;12:1457–1466. [PubMed: 11359935]

Chai Y, Maxson RE Jr. Recent advances in craniofacial morphogenesis. Dev. Dyn 2006;235:2353–2375.

Cuervo R, Valencia C, Chandraratna RA, Covarrubias L. Programmed cell death is required for palate shelf fusion and is regulated by retinoic acid. Dev. Biol 2002;245:145–156. [PubMed: 11969262]

Dudas M, Kaartinen V. Tgf-beta superfamily and mouse craniofacial development: interplay of morphogenetic proteins and receptor signaling controls normal formation of the face. Curr. Top. Dev. Biol 2005;66:65–133.65-133

Dudas M, Kim J, Li WY, Nagy A, Larsson J, Karlsson S, Chai Y, Kaartinen V. Epithelial and ectomesenchymal role of the type I TGF-beta receptor ALK5 during facial morphogenesis and palatal fusion. Dev. Biol 2006;296:298–314. [PubMed: 16806156]

Ferguson MW. Palate development. Development 1988;103(Suppl):41–60. [PubMed: 3074914]

Fitzpatrick DR, Denhez F, Kondaiah P, Akhurst RJ. Differential expression of TGF beta isoforms in murine palatogenesis. Development 1990;109:585–595.

Foitzik K, Paus R, Doetschman T, Dotto GP. The TGF-beta2 isoform is both a required and sufficient inducer of murine hair follicle morphogenesis. Dev. Biol 1999;212:278–289. [PubMed: 10433821]

Gritli-Linde A. Molecular control of secondary palate development. Dev. Biol 2007;301:309–326.

Harlow, E.; Lane, D. A Laboratory Manual. CSH Press; New York: 1988. Antibodies.

Hay ED. An overview of epithelio-mesenchymal transformation. Acta Anat. (Basel) 1995;154:8–20. [PubMed: 8714286]

Hilliard SA, Yu L, Gu S, Zhang Z, Chen YP. Regional regulation of palatal growth and patterning along the anterior-posterior axis in mice. J. Anat 2005;207:655–667.

Hogan, B.; Beddington, R.; Costantini, F.; Lacy, E. A laboratory manual. Cold Spring Harbor Laboratory Press; New York: 1994. Manipulating the mouse embryo.

Kaartinen V, Cui XM, Heisterkamp N, Groffen J, Shuler CF. Transforming growth factor-beta3 regulates transdifferentiation of medial edge epithelium during palatal fusion and associated degradation of the basement membrane. Dev. Dyn 1997;209:255–260.

Kaartinen V, Dudas M, Nagy A, Sridurongrit S, Lu MM, Epstein JA. Cardiac outflow tract defects in mice lacking ALK2 in neural crest cells. Development 2004;131:3481–3490.

Kaartinen V, Voncken JW, Shuler C, Warburton D, Bu D, Heisterkamp N, Groffen J. Abnormal lung development and cleft palate in mice lacking TGF-beta 3 indicates defects of epithelial-mesenchymal interaction. Nat. Genet 1995;11:415–421.

Kulkarni AB, Huh CG, Becker D, Geiser A, Lyght M, Flanders KC, Roberts AB, Sporn MB, Ward JM, Karlsson S. Transforming growth factor beta 1 null mutation in mice causes excessive inflammatory response and early death. Proc. Natl. Acad. Sci. U. S. A 1993;90:770–774.

Li J, Foitzik K, Calautti E, Baden H, Doetschman T, Dotto GP. TGF-beta3, but not TGF-beta1, protects keratinocytes against 12-O- tetradecanoylphorbol-13-acetate-induced cell death in vitro and in vivo. J. Biol. Chem 1999;274:4213–4219. [PubMed: 9933619]

Martinez-Alvarez C, Bonelli R, Tudela C, Gato A, Mena J, O'Kane S, Ferguson MW. Bulging medial edge epithelial cells and palatal fusion. Int. J. Dev. Biol 2000;44:331–335.

Moorman AF, Houweling AC, de Boer PA, Christoffels VM. Sensitive nonradioactive detection of mRNA in tissue sections: novel application of the whole-mount in situ hybridization protocol. J. Histochem. Cytochem 2001;49:1–8.

Murray JC. Gene/environment causes of cleft lip and/or palate. Clin. Genet 2002;61:248–256.

Nawshad A, Lagamba D, Hay ED. Transforming growth factor beta (TGFbeta) signalling in palatal growth, apoptosis and epithelial mesenchymal transformation (EMT). Arch. Oral Biol 2004;49:675–689.

Nawshad A, Lagamba D, Polad A, Hay ED. Transforming growth factor-beta signaling during epithelial-mesenchymal transformation: implications for embryogenesis and tumor metastasis. Cells Tissues. Organs 2005;179:11–23.

Pelton RW, Dickinson ME, Moses HL, Hogan BL. In situ hybridization analysis of TGF beta 3 RNA expression during mouse development: comparative studies with TGF beta 1 and beta 2. Development 1990;110:609–620.

Proetzel G, Pawlowski SA, Wiles MV, Yin M, Boivin GP, Howles PN, Ding J, Ferguson MW, Doetschman T. Transforming growth factor-beta 3 is required for secondary palate fusion. Nat. Genet 1995;11:409–414.

Rice DP. Craniofacial anomalies: from development to molecular pathogenesis. Curr. Mol. Med 2005;5:699–722. [PubMed: 16305494]

Roberts AB, Sporn MB. Differential expression of the TGF-beta isoforms in embryogenesis suggests specific roles in developing and adult tissues. Mol. Reprod. Dev 1992;32:91–98.

Sanford LP, Ormsby I, Gittenberger-de Groot AC, Sariola H, Friedman R, Boivin GP, Cardell EL, Doetschman T. TGFbeta2 knockout mice have multiple developmental defects that are non-overlapping with other TGFbeta knockout phenotypes. Development 1997;124:2659–2670.

Schutte BC, Murray JC. The many faces and factors of orofacial clefts. Hum. Mol. Genet 1999;8:1853–1859.

Shah M, Foreman DM, Ferguson MW. Neutralisation of TGF-beta 1 and TGF-beta 2 or exogenous addition of TGF-beta 3 to cutaneous rat wounds reduces scarring. J. Cell Sci 1995;108(Pt 3):985–1002.

Shi W, Heisterkamp N, Groffen J, Zhao J, Warburton D, Kaartinen V. TGF-beta3-null mutation does not abrogate fetal lung maturation in vivo by glucocorticoids. Am. J. Physiol 1999;277:L1205–L1213.

Shuler CF. Programmed cell death and cell transformation in craniofacial development. Crit Rev. Oral Biol. Med 1995;6:202–217. [PubMed: 8785261]

Shull MM, Ormsby I, Kier AB, Pawlowski S, Diebold RJ, Yin M, Allen R, Sidman C, Proetzel G, Calvin D. Targeted disruption of the mouse transforming growth factor-beta 1 gene results in multifocal inflammatory disease. Nature 1992;359:693–699. [PubMed: 1436033]

Taya Y, O'Kane S, Ferguson MW. Pathogenesis of cleft palate in TGF-beta3 knockout mice. Development 1999;126:3869–3879.

Xu X, Han J, Ito Y, Bringas P Jr. Urata MM, Chai Y. Cell autonomous requirement for Tgfbr2 in the disappearance of medial edge epithelium during palatal fusion. Dev. Biol 2006;297:238–248. [PubMed: 16780827]

Young DL, Schneider RA, Hu D, Helms JA. Genetic and teratogenic approaches to craniofacial development. Crit Rev. Oral Biol. Med 2000;11:304–317.

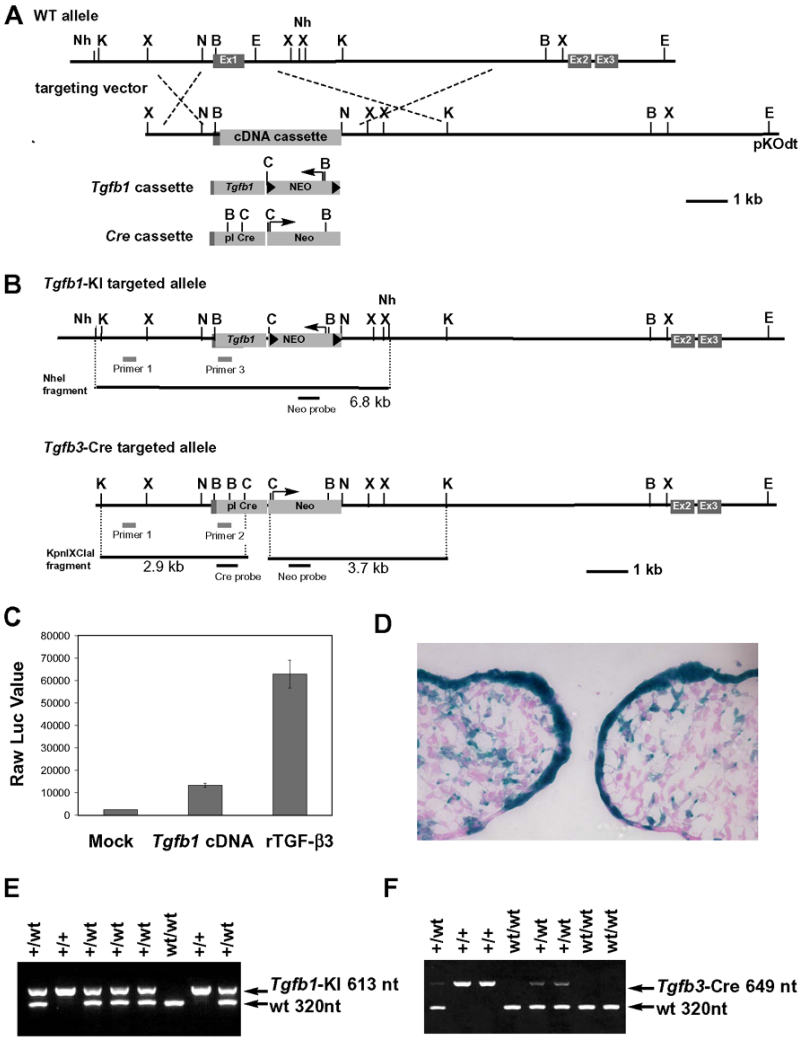

Fig. 1. Generation of *Tgfb1* knockin and Cre knockin mice

(A) A schematic diagram of *Tgfb3* allele and targeting vectors for *Tgfb1* knockin (*Tgfb1*-KI) and Cre knockin (*Tgfb3*-Cre). Ex1, Ex2, Ex3: Exon1, Exon2, and Exon3; *Tgfb1* cassette: *Tgfb1* cDNA with phosphoglycerate kinase polyA sequence and the *pgk* promoter driven neomycin-resistant gene flanked by loxP sites; Cre cassette: the promotorless Cre gene with the neomycin-resistant gene driven by the *pgk* promoter; Nh: NheI, K: KpnI, X: XhoI, B: BamHI, E: EcoRI, C: ClaI, N: NotI. (B) A schematic diagram for the targeted alleles. PCR and Southern blot screening strategies are illustrated. (C) Luciferase reporter assay for PCR-amplified *Tgfb1* cDNA. MLE cells stably integrated with plasminogen activator inhibitor-1/luciferase reporter plasmid were cultured with supernatants from mock transfected cells (Mock) or *Tgfb1* cDNA expression plasmid-transfected cells (*Tgfb1* cDNA). The supernatant containing recombinant TGF-β3 at 10 ng/ml served as a positive control (rTGF-β3). Data are presented as raw luciferase values against each supernatant, n=2. (D) A lineage tracing assay for *Tgfb3* expressing cells in the prefusion palate at E14: X-gal staining of the frontal frozen section from *Tgfbr3-Cre+/−;R26R+/−* embryos. (E-F) Genotyping of *Tgfb1*-KI and *Tgfb3*-Cre mice using PCR analysis.

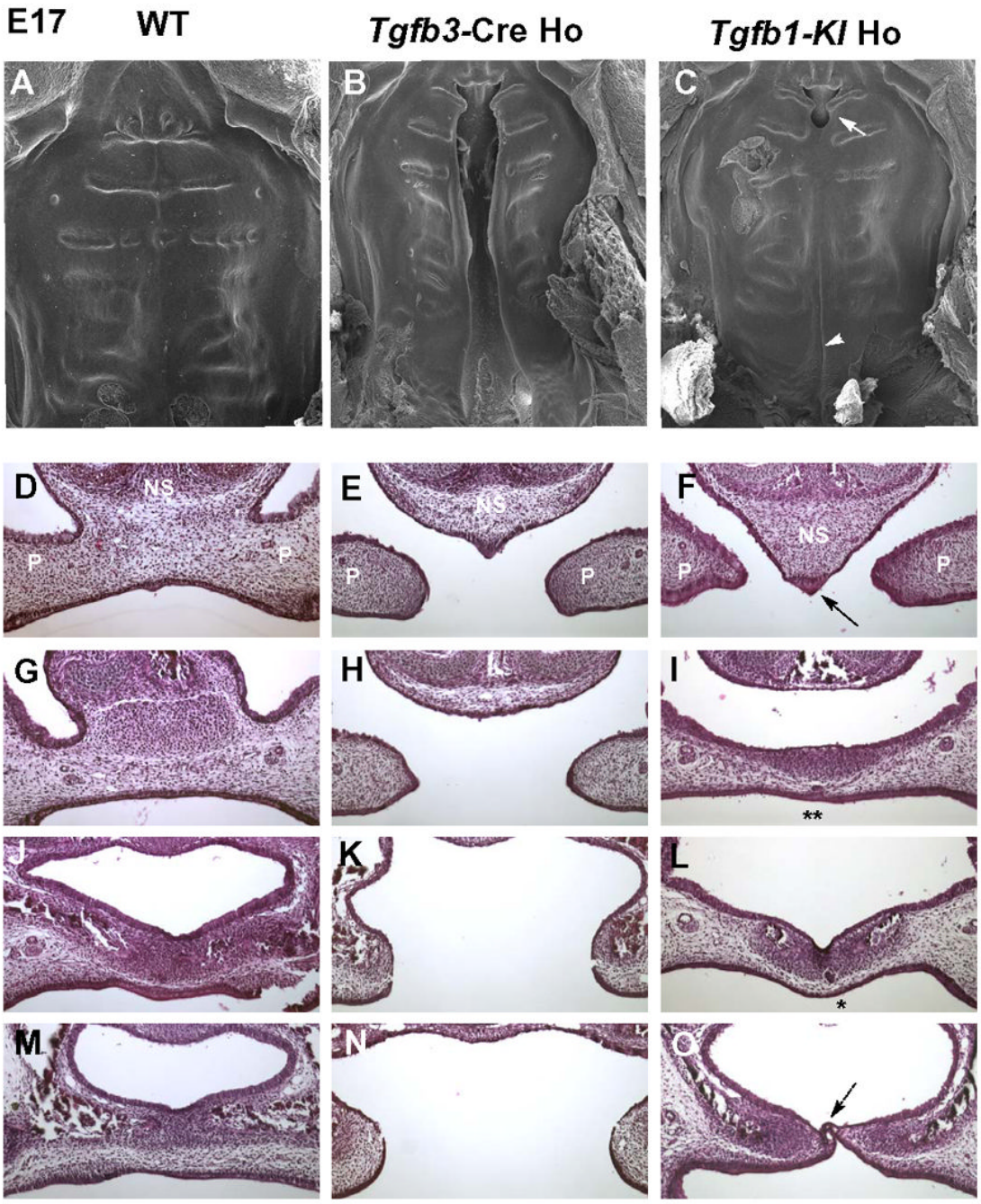

Fig. 2. Scanning electron microscopic and histological analyses of palates from wildtype, *Tgfb3*-Cre homozygote, and *Tgfb1* knockin homozygote embryos.

(A-C) Scanning electron microscopic images of palate from wildtype (WT), *Tgfb3-Cre* homozygote (*Tgfb3*-Cre Ho), and *Tgfb1* knockin homozygote (*Tgfb1*KI Ho) mice at E17. A wildtype specimen displays a fully fused palate. *Tgfb3*-Cre homozygote mouse exhibits a complete bilatateral clefting of the secondary palate, whereas the *Tgfb1*-KI homozygote mouse only has a cleft on the junction of primary and secondary palate (arrow) and a submucous cleft in the posterior region (arrowhead). (D-O) Samples from E17 embryos were sectioned serially in the frontal orientation and stained by hematoxylin-eosin. Sections at four different levels are shown for wildtype (D, G, J, M), *Tgfb3-Cre* Ho (E, H, K, N), and *Tgfb1*-KI Ho (F, I, L, O)

embryos. In the *Tgfb1*-KI homozygote sample, the nasal septum fails to fuse with palatal shelves in the anterior region of the palate (F, arrow); palatal shelves fused in the middle region of the palate with the epithelial islands (I, L; single and double stars), indicating an ongoing process of palatal fusion; a submucous cleft is present in the posterior region of the palate (O, dotted arrow). In the wildtype sample, the palatal shelves demonstrate a complete fusion. In the *Tgfb3* knockout sample, the palatal shelves display a failure to fuse along the anterior-posterior axis. NS: nasal septum; P: palatal shelf.

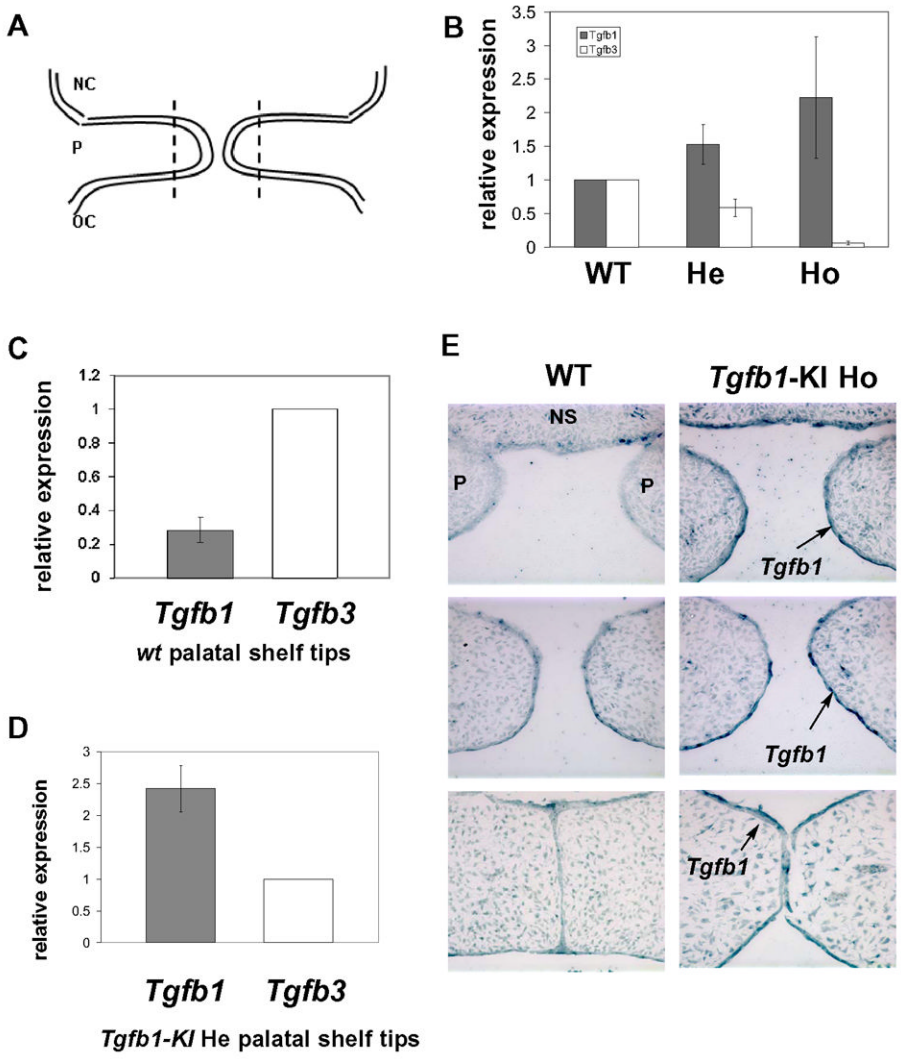

Fig. 3. Gene expression analyses of the *Tgfb1* knock-in mice

(A) A schematic presentation of prefusion palatal shelves. Distal tips of prefusion palatal shelves to be dissected for real-time PCR analysis are indicated by a dotted line. NC: nasal cavity, P: palatal shelf, OC: oral cavity. (B) Real-time quantitative PCR analysis for the expression of *Tgfb1* and *Tgfb3* in tips of palatal shelves dissected from wildtype (WT), *Tgfb1*-KI heterozygous (He), and *Tgfb1*KI homozygous (Ho) embryos at E14. In embryos heterozygous for the *Tgfb1*-KI allele, there is a 50% decrease in *Tgfb3* expression and a concomitant 50% increase in *Tgfb1* expression when compared to the wild-type sample. In embryos homozygous for the *Tgfb1*-KI allele, *Tgfb3* expression is barely detectable, while expression of *Tgfb1* has increased 2-fold when compared to the wild-type sample. Bar graph: mean +/− s.d., n=3; The expression level of *Tgfb1* and *Tgfb3* in the wildtype specimen has been arbitrarily set at 1; results shown are from three independent litters. (C) Real-time absolute quantitative PCR analysis for gene expression of *Tgfb1* and *Tgfb3* in the tips of wildtype (WT) prefusion palatal shelves at E14. Bar graph: mean +/-s.d., n=4; *Tgfb3* expression has been arbitrarily set at 1. (D) Real-Time absolute quantitative PCR analysis for the expression level of *Tgfb1* and *Tgfb3* in tips of palatal shelves dissected from *Tgfb1*KI heterozygotes at E14. Bar graph: mean +/− s.d., n=5; *Tgfb3* expression has been arbitrarily set at 1. (E) *In situ* hybridization for *Tgfb1* in the prefusion palatal shelves of the wild-type and *Tgfb1*-KI

homozygote embryos (n=3). E14 embryos were processed for serial sectioning in a transverse orientation. Sections from the anterior, the middle, and the posterior region of the palate were hybridized with the *Tgfb1* anti-sense probe. The palatal epithelium shows a strong *Tgfb1* hybridization signal along the entire anterior-posterior axis (arrow).

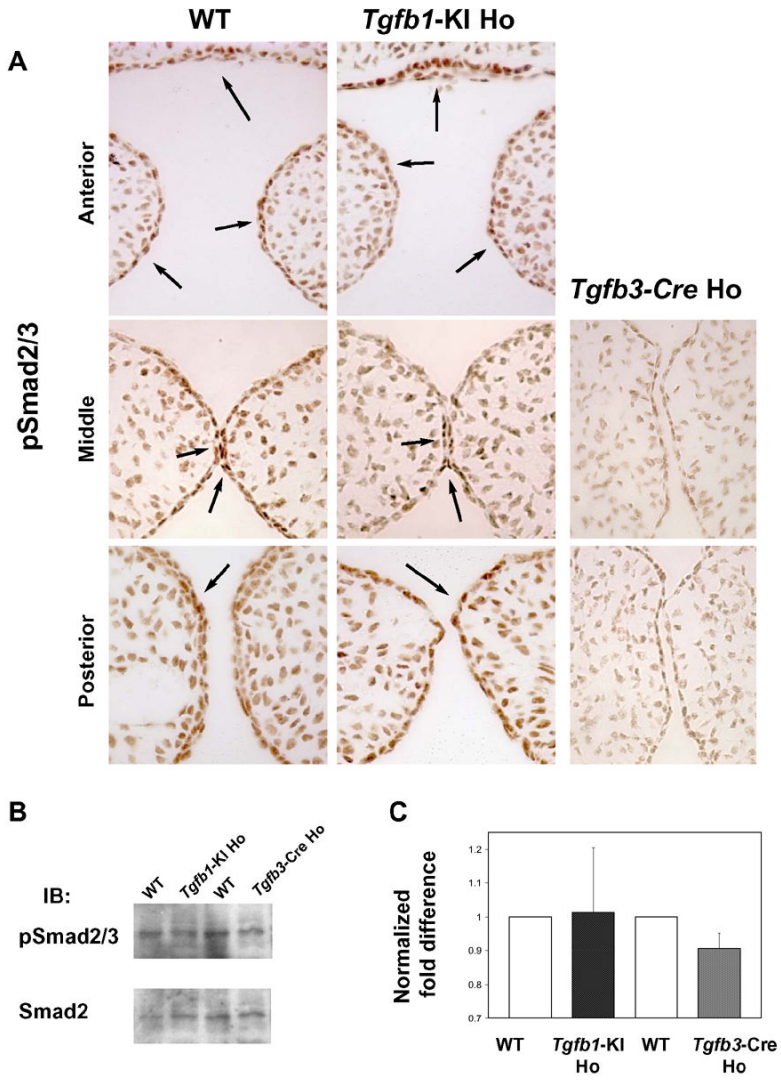

Fig. 4. Comparison of the phospho-Smad2/3 state in the midline palatal epithelium

A, Paraffin sections from wild-type (left panel), *Tgfb3*-Cre homozygote (*Tgfb3*-Cre Ho, right panel), and *Tgfb1*-KI homozygote (*Tgfb1*-KI Ho, mid panel) were immunostained with a phospho-specific antibody against phosphorylated Smad2 and Smad3 (anterior to posterior from top to bottom). In wild-type and *Tgfb1*-KI Ho samples, cells in the periderm, palatal epithelium and in the nasal septum (epithelium) display a strong positive signal (arrows left and mid panels), whereas in the *Tgfb3*-Cre sample (right panel) the pSmad2/3 staining is undetectable (n=3).

B, Tissues harvested from tips of prefusion palatal shelves were analyzed for Smad2/3 phosphorylation using western blotting with anti-phopho-Smad2/3 antibodies. C, The histogram represents the relative quantitation of the scanned images. The wild-type (control) phospho-Smad2/3 to Smad2/3 ratio was arbitrarily set at 1 (n=3).

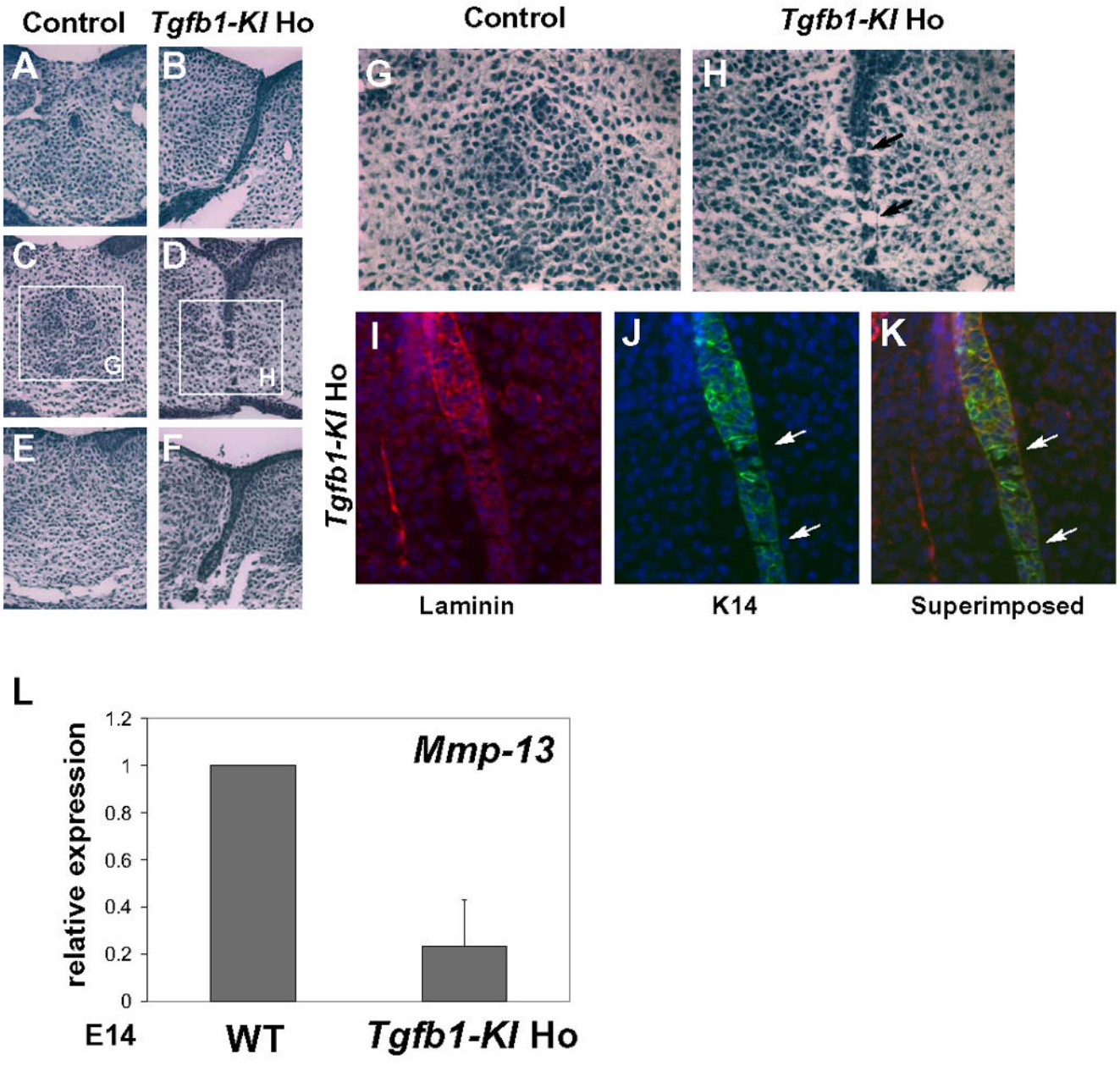

Fig. 5. Comparison of the palatal fusion between *Tgfb1-KI* homozygote and control embryos *in vitro*

Prefusion palatal shelves were dissected from E14 embryos, cultured under chemically defined conditions for 48 hours and analyzed using serial sectioning. Wildtype (A, C, E) and *Tgfb1-KI* homozygote (B, D, F) samples were sectioned at three different levels and stained with hematoxylin & eosin. (G, H), higher magnification of the rectangular regions indicated in the (C, D). In control samples, the midline seam disappears with only a few epithelial islands left, indicating an almost complete fusion (G). In *Tgfβ1-KI* homozygous samples, the midline seam is in the process of breaking down, displaying a patchy loss of epithelial cells (H). The basement membrane is visible even at sites where the epithelial seam is breaking down (arrows in H). (I-K) Paraffin-sections from the palatal shelf organ culture of *Tgfb1*-KI homozygote were immunostained for laminin (M) and K14 (N). The superimposed image is shown in (K). Arrows

in (J) and (K) point out the breakdown of the midline epithelial seam. (L) Real-time quantitative PCR analysis of M*mp-13* expression in tips of palatal shelves dissected from wild-type (WT) and *Tgfb1*-KI homozygote (*Tgfb1*-KI Ho) embryos at E14. *Mmp-13* expression in the *Tgfb1*KI homozygote is about 30% of that expressed in the wild-type. Bar graph: mean +/−s.d., n=3; WT level has been arbitrarily set at 1.

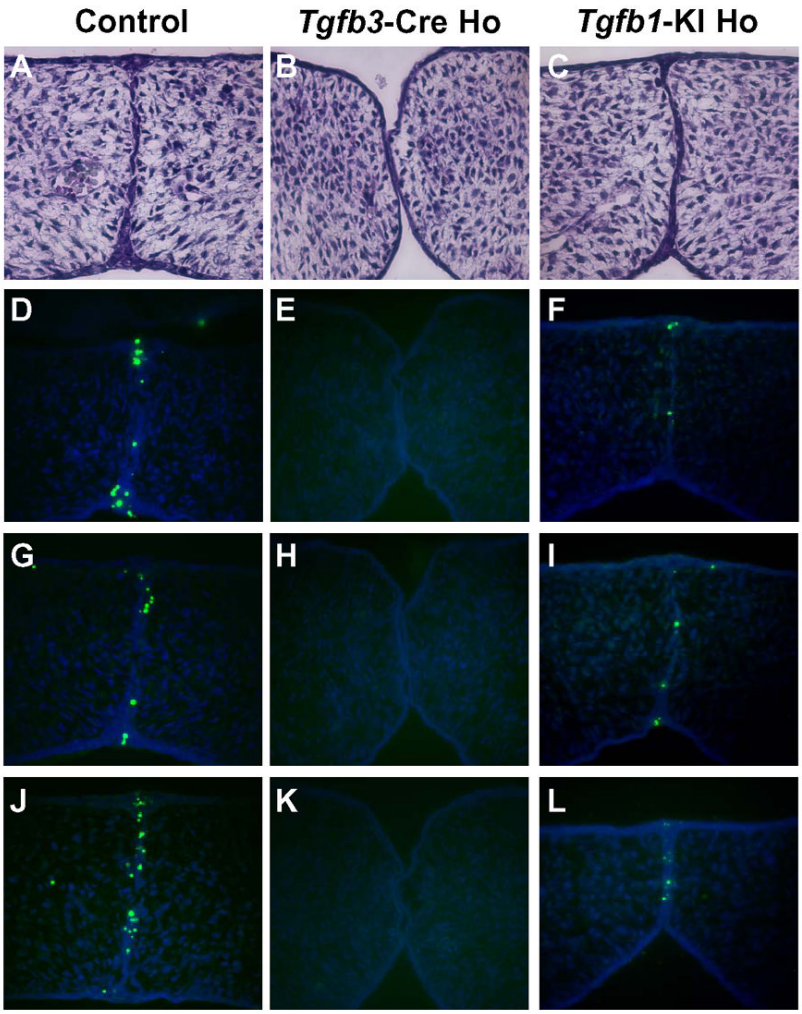

Fig. 6. Histological analysis and TUNEL assays on palatal shelves from control, *Tgfb3*-Cre homozygote, and *Tgfb1*-KI homozygote mice

Embryos of each genotype indicated were harvested at E14 and sectioned serially (frontal orientation). (A-C) Histological analysis of frontal sections at comparable levels, staining with hematoxylin & eosin. Palatal shelves of *Tgfb3*-Cre homozygote made contact but failed to adhere and form epithelial triangles (B). In contrast, palatal shelves of the *Tgfb1*-KI homozygote (C) were adherent and formed epithelial triangles, which were similar to those from the control sample (A). (D-L) TUNEL assays on frontal sections at three different levels from each genotype (n=3). The *Tgfb1*-KI homozygote sample (F, I, L) exhibits a reduced number of apoptotic cells when compared to a control (D, G, J). Apoptotic cells were undetectable in the midline epithelium of the *Tgfb3*-Cre homozygote sample (E, H, K).